

## DESIGN OF ADVANCED RESOLVER-TO-DIGITAL CONVERTERS

F. Auger<sup>1</sup>, O. Mansouri – Toudert<sup>2</sup>, A. Chibah<sup>1</sup>,

1. IREENA Pôle Énergie, CRTT, 37 Bd de l'Université, BP 406, 44602 Saint-Nazaire cedex, France

e-mail : [francois.auger@univ-nantes.fr](mailto:francois.auger@univ-nantes.fr), [arezki.chibah@etu.univ-nantes.fr](mailto:arezki.chibah@etu.univ-nantes.fr)

web : <http://www.univ-nantes.fr/auger-f>

2. Département Électrotechnique de la Faculté de Génie Électrique et Informatique,  
Université Mouloud Mammeri de Tizi-Ouzou, Algérie

e-mail : [toudert.ouiza@yahoo.fr](mailto:toudert.ouiza@yahoo.fr)

**Abstract** - Absolute position sensors such as resolvers or magnetic encoders are sometimes used in motor control applications. They require a particular processing of their two output signals to provide some estimations of the rotor position and of the rotor speed. The first aim of this paper is to recall the basic principle, the performance and the implementation issues of the most common angle tracking observers. Two improved versions are then proposed: a third-order continuous-time Luenberger observer and a third-order discrete-time extended Kalman filter.

**Keyword** - absolute position sensors, resolvers, magnetic encoders, Luenberger observers, Kalman filters.

### 1 INTRODUCTION

In several cases, the measurement of the shaft position of a motor is derived from two analog signals that are proportional to the sine and cosine of the shaft rotation angle. Such a case can be found for example

- when a resolver is used. Compared to other absolute position sensors, a resolver can be used for high speed measurements, yields a high accuracy, has small size, low weight, low moment of inertia, high noise immunity and low sensitivity to mechanical deformations. Some people say that compared to all the absolute position sensors, resolvers are the most robust and stable in long-term performance [6]. Its AC output signals allow an efficient data transmission over long distances (up to 2 km with suitable cables) [9]. Resolvers can be considered as rotary transformers with an excitation winding on the rotor, which is magnetically coupled with two identical stator windings placed 90° apart (see Fig. 1). These sensors are used extensively in machine tools, elevators, radars and aircraft on board instrument systems.
- when a magnetic position encoder is used [18, 20]. This kind of sensor uses a steel target wheel with teeth and slots that produce modulations of the flux from a stationary magnet that can be read by Hall sensors or magnetoresistors. It is commonly used in automotive applications facing the challenges of high temperature and large air gaps, because it has a simple and ro-

bust structure, low power requirements and an excellent resistance to humid and dirty environments [18].

- when using balanced three-phase high frequency signal injection for sensorless control of salient AC machines. This approach consists in superimposing a high frequency test signal on the stator voltage and to recover the rotor position information from the stator currents [4, 17].

To estimate the rotor position from these analog signals, a resolver-to-digital converter is used. This signal processing task generally estimates both the rotor angular position and the rotor speed.

### 2 CONTINUOUS-TIME DESIGNS

#### 2.1 THE CLASSICAL ANGLE TRACKING OBSERVER

The most simple angle tracking observer is derived from a linear second-order continuous-time state space model of the angular position:

$$\dot{X}(t) = A_1 X(t) + G_1 \alpha(t), \text{ with } X = \begin{pmatrix} \theta \\ \Omega \end{pmatrix}, \quad (1)$$

$$y_1(t) = C_1 X(t) + w(t), \text{ with } \Omega = \dot{\theta} \quad (2)$$

$$\text{with } A_1 = \begin{pmatrix} 0 & 1 \\ 0 & 0 \end{pmatrix}, C_1^T = \begin{pmatrix} 1 \\ 0 \end{pmatrix} \text{ and } G_1 = \begin{pmatrix} 0 \\ 1 \end{pmatrix},$$

where  $\dot{X}$  is the derivative of  $X$ . The process output  $y_1$  is considered as a noisy measurement of the true position  $\theta$ , blurred with an additive zero-mean noise  $w$ . The angular acceleration  $\alpha(t) = \dot{\Omega}(t) = \ddot{\theta}(t)$  is considered as a zero-mean state noise. Since this

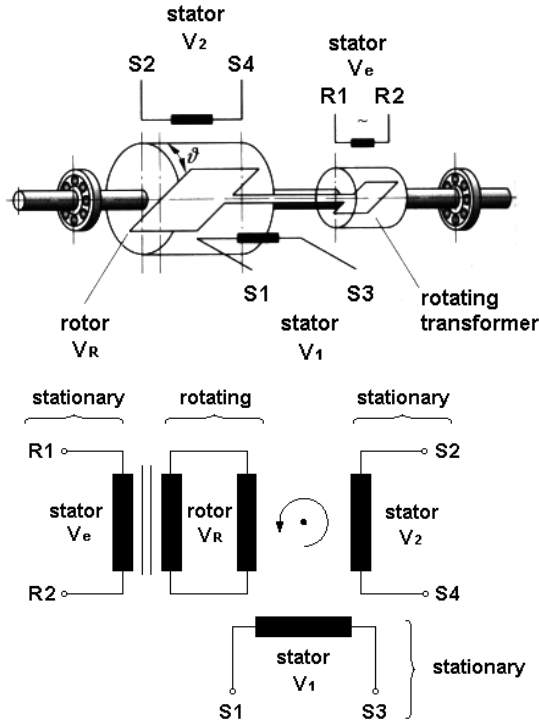


Fig. 1. Basic principle of a resolver (source:<http://data.bolton.ac.uk/mind>).

stochastic process is observable [24], a Luenberger observer [8] can be used

$$\dot{\hat{X}}(t) = A_1 \hat{X}(t) + K_{c1}(y_1(t) - C_1 \hat{X}(t)) \quad (3)$$

$$\text{with } K_{c1}^T = (k_{a1} \ k_{b1}) \text{ and } \hat{X}^T = (\hat{\theta} \ \hat{\Omega})$$

The estimation error of this observer converges to zero provided that  $k_{a1} > 0$  and  $k_{b1} > 0$ . This observer is equivalent to an integrator in closed loop with a PI controller [3, 14, 15, 21] with proportional gain  $K_p = k_{a1}$  and integral time  $T_i = k_{a1}/k_{b1}$  (see Fig. 2). The transfer functions of this filtering process applied to the measured signal  $y_1(t)$ ,

$$\hat{\Theta}(s) = \frac{k_{a1}s + k_{b1}}{s^2 + k_{a1}s + k_{b1}} Y_1(s) \quad (4)$$

$$\hat{\Omega}(s) = \frac{k_{b1}s}{s^2 + k_{a1}s + k_{b1}} Y_1(s) \quad (5)$$

corresponds for  $\hat{\Theta}(s)$  to a second-order low-pass filter with a static gain equal to 1 and a slope at high frequencies of only  $-20$  dB/dec. This particular structure yields an unbiased estimation of the position when the position is constant or when the speed is constant: since

$$Y_1(s) - \hat{\Theta}(s) = \frac{s^2}{s^2 + k_{a1}s + k_{b1}} Y_1(s),$$

it can be shown using the final-value theorem that if  $Y_1(s) = \Theta(s) = \frac{\omega}{s^2}$ ,

$$\begin{aligned} \lim_{t \rightarrow +\infty} y_1(t) - \hat{\theta}(t) &= \lim_{s \rightarrow 0} s \left( Y_1(s) - \hat{\Theta}(s) \right) \\ &= \lim_{s \rightarrow 0} s \frac{s^2}{s^2 + k_{a1}s + k_{b1}} \frac{\omega}{s^2} = 0 \end{aligned} \quad (6)$$

However, this position estimator suffers from a tracking error when the speed is linearly increasing:

$$\text{if } Y_1(s) = \frac{\alpha}{s^3}, \lim_{t \rightarrow +\infty} y_1(t) - \hat{\theta}(t) = \frac{\alpha}{k_{b1}} \quad (7)$$

This allows to derive  $k_{b1}$  from the maximum permissible position estimation error for a given angular acceleration  $\alpha$  by the expression  $k_{b1} = \alpha / (\theta_{\text{true}} - \hat{\theta})$  [1]. For example, for a machine with a maximal electromagnetic torque equal to  $T_e = 50$  N.m and a total moment of inertia equal to  $J = 10^{-2}$  kg.m<sup>2</sup>, the highest angular acceleration will be  $\alpha = T_e/J = 5000$  rad/s<sup>2</sup>. If the maximum permissible error is 1 degree, then  $k_{b1} = 5000 * 180/\pi \approx 286500$  s<sup>-2</sup>. This parameter  $k_{b1}$  can also be chosen so as to increase the accuracy of the estimator: the smaller  $k_{b1}$ , the smaller the variance of the estimation error. The first coefficient,  $k_{a1}$ , can be chosen equal to  $2m\sqrt{k_{b1}}$ , where  $m$  is a damping ratio. This parameter can be chosen so as to obtain a desired peak overshoot when the actual rotor position changes from 0 to 180°. For example, choosing  $m = 1.945$  will provide an overshoot of 5%. Choosing  $m = \sqrt{2}/2$  (Butterworth case) will lead to an overshoot of 20.84%.

A discrete-time version of this observer can be designed using the discrete-time equivalent model of this continuous-time observer [8, 22],

$$\begin{aligned} e[k] &= y_1[k] - x_1[k] \\ x_1[k+1] &= x_1[k] + x_2[k] + k_{a1} T_s e[k] \\ x_2[k+1] &= x_2[k] + k_{b1} T_s^2 e[k] \end{aligned} \quad (8)$$

where  $T_s$  is the sampling period,  $x_1[k] = \hat{\theta}(kT_s)$  and  $x_2[k] = T_s \hat{\Omega}(kT_s)$ . This algorithm only requires 2 multiplications and 4 additions per iteration.

When the position measurement system yields two signals deduced from the sine and cosine of the rotor position,  $y_c(t) = \cos(\theta(t)) + w_c(t)$  and  $y_s(t) = \sin(\theta(t)) + w_s(t)$ ,  $w_c(t)$  and  $w_s(t)$  being two additive zero-mean noises of equal variance, The resulting nonlinear dynamic process remains observable. The error term  $e(t) = y_1(t) - \hat{\theta}(t)$  used in eq. 3 is simply replaced by

$$\begin{aligned} \epsilon(t) &= y_s(t) \cos(\hat{\theta}(t)) - y_c(t) \sin(\hat{\theta}(t)) \\ &= \sin(\theta(t) - \hat{\theta}(t)) \\ &\quad + w_s(t) \cos(\hat{\theta}(t)) - w_c(t) \sin(\hat{\theta}(t)) \end{aligned} \quad (9)$$

The resulting observer remains stable [12].

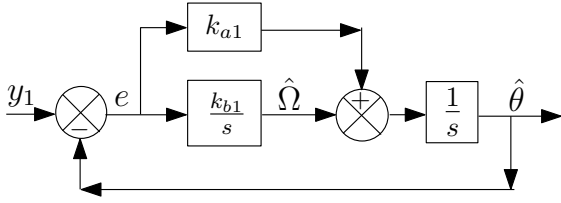


Fig. 2. Block diagram of a classical angle tracking observer. The localisation of  $\hat{\Omega}$  in this block-diagram deserves attention.

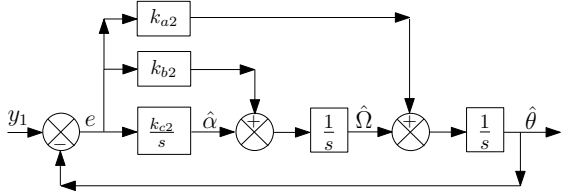


Fig. 3. Block diagram of the first angle tracking observer proposed in this paper.

## 2.2 AN IMPROVED CONTINUOUS-TIME ATO

To obtain better transients during startup (or more generally when the speed is not constant), one possibility is to use a third-order continuous-time state space model of the angular position:

$$\dot{X}(t) = A_2 X(t) + G_2 \beta(t), \text{ with } X = \begin{pmatrix} \theta \\ \Omega \\ \alpha \end{pmatrix} \quad (10)$$

$$y_1(t) = C_2 X(t) + w(t), \quad (11)$$

$$A_2 = \begin{pmatrix} 0 & 1 & 0 \\ 0 & 0 & 1 \\ 0 & 0 & 0 \end{pmatrix}, C_2^T = \begin{pmatrix} 1 \\ 0 \\ 0 \end{pmatrix} \text{ and } G_2 = \begin{pmatrix} 0 \\ 0 \\ 1 \end{pmatrix},$$

where the angular jerk  $\beta(t) = \dot{\alpha}(t) = \ddot{\Omega}(t) = \ddot{\theta}(t)$  is considered as a zero-mean state noise. Since this stochastic process is also observable, a Luenberger observer can be used to estimate  $\theta$  and  $\Omega$ :

$$\dot{\hat{X}}(t) = A_2 \hat{X}(t) + K_{c2} (y_1(t) - C_2 \hat{X}(t)) \quad (12)$$

$$\text{with } K_{c2}^T = (k_{a2} \ k_{b2} \ k_{c2}) \text{ and } \hat{X}^T = (\hat{\theta} \ \hat{\Omega} \ \hat{\alpha})$$

Using the Routh-Hurwitz criterion, it can be shown that the estimation error of this new observer converges to zero provided that  $k_{a2} k_{b2} > k_{c2}$ . This position estimator can be written as

$$\hat{\Theta}(s) = \left[ k_{b2} + \frac{k_{c2}}{s} + k_{a2} s \right] \frac{1}{s^2} (Y_1(s) - \hat{\Theta}(s))$$

This result shows that this observer is equivalent to a double integrator in closed loop with a PID controller with proportional gain  $K_p = k_{b2}$ , integral time  $T_i = \frac{k_{b2}}{k_{c2}}$  and derivative time  $T_d = \frac{k_{a2}}{k_{b2}}$ . This

results also shows that the proposed estimator is very closed to the one proposed in [7], but without using a correction derived from the electrical model of a machine. Fig. 3 shows an efficient implementation of this estimator. The transfer functions of this filtering process applied to the measured signal  $y_1(t)$ ,

$$\hat{\Theta}(s) = \frac{k_{a2} s^2 + k_{b2} s + k_{c2}}{s^3 + k_{a2} s^2 + k_{b2} s + k_{c2}} Y_1(s) \quad (13)$$

$$\hat{\Omega}(s) = \frac{(k_{b2} s + k_{c2}) s}{s^3 + k_{a2} s^2 + k_{b2} s + k_{c2}} Y_1(s) \quad (14)$$

$$\hat{\alpha}(s) = \frac{k_{c2} s^2}{s^3 + k_{a2} s^2 + k_{b2} s + k_{c2}} Y_1(s) \quad (15)$$

corresponds for  $\hat{\Theta}(s)$  to a third-order low-pass filter with, once again, a static gain equal to 1 and a slope at high frequencies of only  $-20$  dB/dec. This structure yields an unbiased estimation of the position when the position is constant, when the speed is constant and also when the acceleration is constant: if  $Y_1(s) = \Theta(s) = \frac{\alpha}{s^3}$ , since

$$Y_1(s) - \hat{\Theta}(s) = \frac{s^3}{s^3 + k_{a2} s^2 + k_{b2} s + k_{c2}} Y_1(s),$$

$$\begin{aligned} \lim_{t \rightarrow +\infty} y_1(t) - \hat{\theta}(t) &= \lim_{s \rightarrow 0} s (Y_1(s) - \hat{\Theta}(s)) \\ &= \lim_{s \rightarrow 0} s \frac{s^3}{s^3 + k_{a2} s^2 + k_{b2} s + k_{c2}} \frac{\alpha}{s^3} = 0 \end{aligned}$$

To choose the coefficients of the observer, one possibility is to choose the poles of the transfer function  $\hat{\Theta}(s)/Y_1(s)$  (eq. 13) as  $-K/T$ ,  $-1/T + j\psi/T$ ,  $-1/T - j\psi/T$ , where  $T$ ,  $K$  and  $\psi$  respectively provide the desired settling time (and the estimation accuracy), the desired peak overshoot and the desired frequency of oscillation. This leads to the following expressions of the observer coefficients:

$$k_{a2} = \frac{K+2}{T}, \quad k_{b2} = \frac{\psi^2 + 2K + 1}{T^2}, \quad k_{c2} = \frac{K(\psi^2 + 1)}{T^3}$$

Choosing  $\psi = 3\pi/2$  and  $K = 39.04$  for example leads to a peak overshoot of 10 %. If the observer coefficients are chosen as  $k_{a2} = 2/T_c$ ,  $k_{b2} = 2/T_c^2$ ,  $k_{c2} = 1/T_c^3$ , where  $T_c$  is a time constant providing the desired settling time, then the denominator of eq. 13 will be a third-order Butterworth filter [5]. The overshoot will then be equal to 30.9 %.

A discrete-time version of this observer can be designed using the discrete-time equivalent model of this continuous-time observer [8, 22],

$$e[k] = y_1[k] - x_1[k] \quad (16)$$

$$x_1[k+1] = x_1[k] + x_2[k] + x_3[k]/2 + k_{a2} T_s e[k]$$

$$x_2[k+1] = x_2[k] + x_3[k] + k_{b2} T_s^2 e[k]$$

$$x_3[k+1] = x_3[k] + k_{c2} T_s^3 e[k]$$

with  $x_1[k] = \hat{\theta}(kT_s)$ ,  $x_2[k] = T_s \hat{\Omega}(kT_s)$  and  $x_3[k] = T_s^2 \hat{\alpha}(kT_s)$ . This algorithm requires 3 multiplications and 7 additions per iteration. This means that compared to the cost of the second-order observer (Eq. 8), the additional cost for a better position estimation during transients is only 1 multiplication and 3 additions.

### 2.3 PHASE UNWRAPPING POSSIBILITIES

When used with a resolver or with a magnetic encoder, the estimated position  $\hat{\theta}(t)$  is generally constrained to lie between 0 and  $2\pi$ . But this constraint is not necessary, and such an observer can also be used to perform phase unwrapping [16, 23]. In some cases, such as in sensorless control of salient PMSM machines by high frequency signal injection,  $\theta = 2\psi$ , where  $\psi$  is the angle to be estimated. The output of the proposed observer  $\hat{\theta}$ , can be constrained to lie between 0 and  $4\pi$ , and then divided by 2.

## 3 DISCRETE-TIME DESIGNS

Another possibility is to derive a state estimator from a discrete-time model of the process [13]. If the chosen states are  $x_1[k] = \theta(kT_s)$ ,  $x_2[k] = T_s \Omega(kT_s)$  and  $x_3[k] = T_s^2 \alpha(kT_s)$ , a state space model derived from a third-order Taylor approximation of the position [2] writes

$$\begin{aligned} X[k+1] &= A_3 X[k] + G v[k] & (17) \\ Y[k+1] &= \begin{pmatrix} y_c[k+1] \\ y_s[k+1] \end{pmatrix} = \mathcal{H}(X[k+1]) + W[k+1], \\ \text{with } X[k] &= \begin{pmatrix} x_1[k] \\ x_2[k] \\ x_3[k] \end{pmatrix}, A_3 = \begin{pmatrix} 1 & 1 & 1/2 \\ 0 & 1 & 1 \\ 0 & 0 & 1 \end{pmatrix}, \\ G^T &= (1/6 \quad 1/2 \quad 1), v[k] = T_s^3 \beta(kT_s), \\ \mathcal{H}(X[k]) &= \begin{pmatrix} \cos(x_1[k]) \\ \sin(x_1[k]) \end{pmatrix} \text{ and } W[k] = \begin{pmatrix} w_c[k] \\ w_s[k] \end{pmatrix} \end{aligned}$$

where the state noise  $v[k]$  and the measurement noise  $W[k+1]$  are two centered random variables of respective variance  $q$  and  $r I_2$ . The transition equation of this process is linear, whereas the observation equation is nonlinear. As a consequence, the prediction part of the Kalman estimator [10] derived from this model can be simply and rigorously computed as

$$\begin{aligned} X_p[k] &= A_3 X_e[k-1] & (18) \\ P_p[k] &= A_3 P_e[k-1] A_3^T + G G^T q & (19) \end{aligned}$$

where  $X_p[k]$  is a prediction of  $X[k]$  (*a priori* estimation extrapolated from  $X_e[k-1]$ , the estimation of  $X[k-1]$ , thanks to the process model) and  $P_p[k]$  is the corresponding error covariance matrix, measuring the quality of this prediction. The estimation part, defined as [19]

$$Y_p[k] = \mathbb{E}[Y[k]|Y[k-1]] \quad (20)$$

$$\tilde{Y}_p[k] = Y[k] - Y_p[k] \quad (21)$$

$$P_{yy}[k] = \mathbb{E}[\tilde{Y}_p[k] \tilde{Y}_p[k]^t | Y[k-1]] \quad (22)$$

$$P_{xy}[k] = \mathbb{E}[\tilde{X}_p[k] \tilde{Y}_p[k]^t | Y[k-1]] \quad (23)$$

$$K[k] = P_{xy}[k] P_{yy}[k]^{-1} \quad (24)$$

$$X_e[k] = X_p[k] + K[k] \tilde{Y}_p[k] \quad (25)$$

$$P_e[k] = P_p[k] - K[k] P_{yy}[k] K^t[k], \quad (26)$$

requires to know the mean of some nonlinear functions of random variables. Since these averages can not be computed rigorously, they must be approximated. The classical extended Kalman filter [10] is based on a first-order Taylor approximation. This approximation leads to approximate  $\mathbb{E}[f(x)]$  by  $f(\mathbb{E}[x])$ , which is very crude in most cases. In this paper, we will study the improvement obtained by the use of a third-order Taylor expansion of  $y_c$  and  $y_s$  around the predicted position  $\theta_p = X_p[k](1)$ . Removing the time index  $[k]$  and using the shorthand notations  $c_p = \cos(\theta_p)$ ,  $s_p = \sin(\theta_p)$ ,  $\tilde{\theta}_p = \theta - \theta_p$ , the measured signals can hence be approximated as

$$\begin{aligned} y_c &= \cos(\theta) + w_c \\ &= \cos(\theta_p + \theta - \theta_p) + w_c & (27) \\ &\approx c_p - s_p \tilde{\theta}_p - c_p \tilde{\theta}_p^2/2 + s_p \tilde{\theta}_p^3/6 + w_c \end{aligned}$$

$$\begin{aligned} y_s &= \sin(\theta) + w_s \\ &= \sin(\theta_p + \theta - \theta_p) + w_c & (28) \\ &\approx s_p + c_p \tilde{\theta}_p - s_p \tilde{\theta}_p^2/2 - c_p \tilde{\theta}_p^3/6 + w_s \end{aligned}$$

If the prediction error  $\tilde{\theta}_p$  is considered as a Gaussian random variable of zero mean and variance  $\mathbb{E}[\tilde{\theta}_p^2] = P_{p11} = P_p[k](1, 1)$ , then the two components of the predicted value of the measurement vector  $Y_p$  (eq. 20) can be approximated by

$$\mathbb{E}[y_c] \approx y_{cp} = (1 - P_{p11}/2) \cos(\theta_p) \quad (29)$$

$$\mathbb{E}[y_s] \approx y_{sp} = (1 - P_{p11}/2) \sin(\theta_p) \quad (30)$$

Using the expressions of some higher order moments of centered Gaussian random variables,  $\mathbb{E}[\tilde{\theta}_p^{2n+1}] = 0$ ,  $\mathbb{E}[\tilde{\theta}_p^4] = 3 P_{p11}^2$ ,  $\mathbb{E}[\tilde{\theta}_p^6] = 15 P_{p11}^3$ , the covariance matrix of the measurement prediction error  $P_{yy}$  (eq. 22) and the correlation matrix between the state prediction error and the measurement prediction error  $P_{xy}$  (eq. 23) can be approximated as

$$\begin{aligned} P_{yy} &= \begin{pmatrix} a c_p^2 + b s_p^2 + r & -s_p c_p (b - a) \\ -s_p c_p (b - a) & a s_p^2 + b c_p^2 + r \end{pmatrix} \\ P_{xy} &= (1 - P_{p11}/2) \begin{pmatrix} -s_p P_{p11} & c_p P_{p11} \\ -s_p P_{p12} & c_p P_{p12} \\ -s_p P_{p13} & c_p P_{p13} \end{pmatrix} \end{aligned}$$

with  $a = P_{p11}^2/2$  and  $b = P_{p11} (\frac{5}{12} P_{p11}^2 - P_{p11} + 1)$ . One remarkable result is that both  $P_{yy}$  and  $P_{xy}$  can

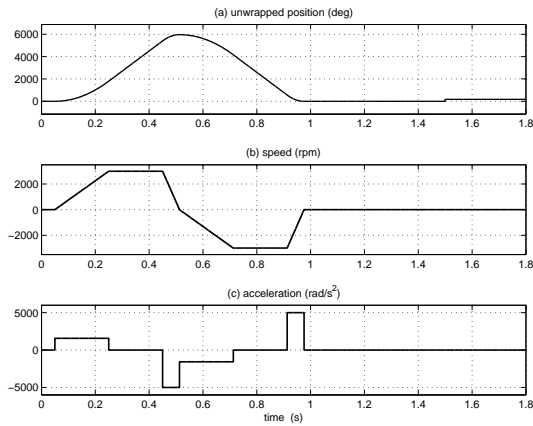


Fig. 4. Absolute position, speed and acceleration of the defined test trajectory.

be factorized as [11]

$$P_{yy} = R D R^T + r \mathbb{I}_2, R = \begin{pmatrix} c_p & -s_p \\ s_p & c_p \end{pmatrix}$$

$$P_{xy} = (1 - P_{p11}/2) P_p H^T R^T$$

with  $H = \begin{pmatrix} 0 & 0 & 0 \\ 1 & 0 & 0 \end{pmatrix}, D = \begin{pmatrix} a & 0 \\ 0 & b \end{pmatrix}$

The main result of this section is that, since  $R^{-1} = R^T$  and  $(A B C)^{-1} = C^{-1} B^{-1} A^{-1}$ , it can be shown that the Kalman gain  $K$  (eq. 24), the covariance matrix of the estimation error  $P_e$  (eq. 26) and the prediction correction  $K \tilde{Y}_p$  (eq. 25) can be written as

$$K = (1 - P_{p11}/2) P_p H^T (D + r \mathbb{I}_2)^{-1} R^T \quad (31)$$

$$= K_{\text{lin}} \begin{pmatrix} -s_p & c_p \end{pmatrix}$$

$$K \tilde{Y}_p = K_{\text{lin}} (y_s c_p - y_c s_p)$$

$$= K_{\text{lin}} (\sin(\theta - \theta_p) + w_s c_p - w_c s_s)$$

$$P_e = P_p - (1 - P_{p11}/2)^2 P_p H^T (D + r \mathbb{I}_2)^{-1} H P_p$$

$$K_{\text{lin}} = \frac{1 - P_{p11}/2}{b + r} P_p C_2^t$$

where  $C_2^t$  is defined in eq. 11. These results show that unlike what usually happens when estimating the state of nonlinear uncertain dynamic systems, the Kalman gain depends on the measured signals only through  $c_p$  and  $s_p$ , and  $P_e$  does not depend on the measured signals. This means that  $K_{\text{lin}}$  goes to a constant limit, and that this apparently complex third-order extended Kalman filter can be reduced to a few elementary equations.

#### 4 CONCLUSIONS

In this paper, some theoretical results have been presented to clarify the properties and the settings of several angle tracking observers. To illustrate these results, some simulations were obtained using a Simulink file which is available on the first author's web site, so as to make these results repro-

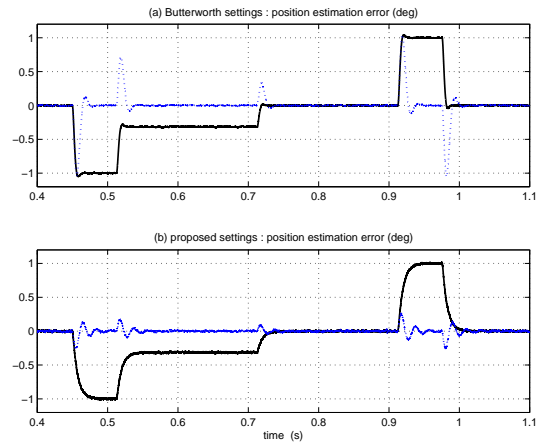


Fig. 5. Position estimation error of the second-order (black solid) and third-order (blue dotted) observers with the Butterworth (a) and the proposed settings (b).

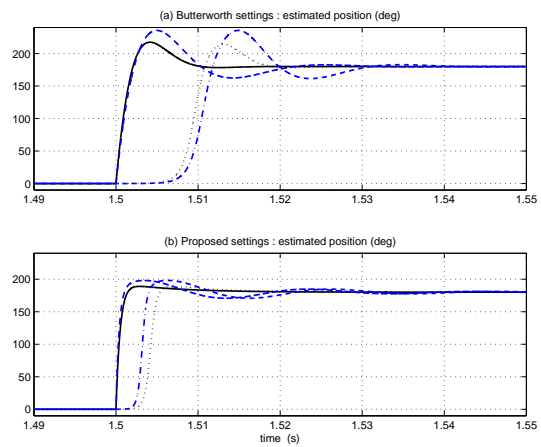


Fig. 6. Estimated position of the second-order observer with a linear (black solid) and with a non-linear measurement (black dotted) and of the third-order observer with a linear (blue dashed) and with a non-linear (blue dash-dotted) measurement.

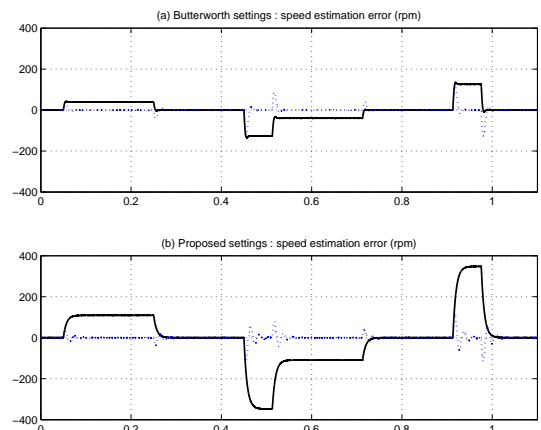


Fig. 7. Speed estimation error of the second-order (black solid) and third-order (blue dotted) observers with the Butterworth (a) and the proposed settings (b).

ducible. To determine the performances of the studied observers (second- and third-order continuous- and discrete-time observers with noisy linear or non-linear measurements), a typical rotor trajectory has been defined (Fig. 4). Fig. 5 shows the position estimation error. When the speed is varying, the second-order observers are biased, whereas the third-order observers are unbiased. The second-order observers have been set such that when the acceleration equals  $5000 \text{ rad/s}^2$ , the error equals 1 degree (see eq. 7). The overshoot is higher for the Butterworth settings than for the proposed ones. Fig. 6 shows the estimated position for an abrupt position change from 0 to 180 degrees. Since the proposed settings are more stiff than the Butterworth settings, the overshoots are lower in the second case. Fig. 6 also evidences that non-linear measurements induce a delayed answer. Fig. 7 shows the speed estimation error. When the acceleration is constant, the bias of the second-order speed estimator is equal to  $\Omega_{\text{true}} - \hat{\Omega} = \alpha k_{a1}/k_{b1} = 2m\alpha/\sqrt{k_{b1}}$ . As a consequence, the higher the damping ratio, the higher the speed estimation error. On the other hand, the simulation results presented on Fig. 7 confirm that the third-order speed estimators are unbiased.

## 5. REFERENCES

- [1] Analog Devices, “AD2S1200: 12-bit R/D converter with reference oscillator”, 2003.
- [2] F. Auger, F. Debrailly, R. Garzon, R. Aubrée, P.-Y. Boisbunon, “Filtrage statistique d’un capteur de position angulaire par filtrage de Kalman : implantation sur microcontrôleur ou sur FPGA à l’aide de bibliothèques jumelles”, *proc. GretsI 2009*, CD-ROM, Dijon, 2009.
- [3] K. Bouallaga, L. Idkhajine, E. Monmasson, A. Prata, “Demodulation methods on fully FPGA-based system for resolver signals treatment”, *proc. EPE’07*, Aalborg (Denmark), 2007.
- [4] M.J. Corley, R.D. Larem, “Rotor position and velocity estimation for a permanent magnet synchronous machine at standstill and high speeds”, *IEEE Trans. on Ind. App.*, Vol. 34, No. 4, pp. 784-789, July-Aug. 1998.
- [5] A.M Davis, “Approximation”, in *The circuits and filters handbook* (W.K. Chen ed.), chap. 66, pp 2161–2191, CRC Press, 1995.
- [6] B. Drury, “The control techniques drives and controls handbook”, The IEE Power and Energy series, Vol 35, CRC Press, 2001.
- [7] G. Ellis, J.O. Kraha, “Observer-based resolver conversion in industrial servo systems”, *proc. PCIM’01 conf.*, CD-ROM, Nuremberg, Germany, 2001.
- [8] B. Friedland, “Observers”, in *The control handbook* (W.S. Levine ed.), chap. 37, pp 607–618, CRC Press, 1996.
- [9] J. Gasking, “Synchro and resolver conversion handbook” North Atlantic Industries, 2005.
- [10] M. Grewal, A.P. Andrews, “Kalman theory, theory and practice using MATLAB (3rd edition)”, Wiley, 2008.
- [11] L. Harnefors, “Speed estimation from noisy resolver signals”, *Proc. Sixth Int. Conf. on Power Electronics and Variable Speed Drives*, pp 279-282, Sept. 1996.
- [12] L. Harnefors, H-P. Nee, “A general algorithm for speed and position estimation of AC motors”, *IEEE Trans. on Industrial Electronics*, Vol. 47, No. 1, pp. 77-83, feb 2000.
- [13] M. Hilaiet, F. Auger, “Speed and position estimation from an absolute position encoder,” *proc. ElectrImacs’99*, pp II-217–222, 1999.
- [14] R. Hoseinnezhad, P. Harding, “A novel hybrid angle tracking observer for resolver to digital conversion” *proc. IEEE CDC-ECC’05 conf.*, pp. 7020-7025, Seville, Spain, 2005.
- [15] L. Idkhajine, “Fully FPGA-based sensorless control for synchronous AC drive using an extended Kalman filter”, PhD thesis, Université de Cergy Pontoise, Nov 24th, 2010.
- [16] K. Itoh, “Analysis of the phase unwrapping problem” *Applied Optics*, Vol. 21, No. 14, p. 2470, July 15, 1982.
- [17] P.L. Jansen, R.D. Lorenz, “Transducerless position and velocity estimation in induction and salient AC machines”, *IEEE Trans. on I.A.*, Vol. 31, No. 2, pp. 240–247, March 1995.
- [18] B. Lequesne, T. Schroeder, “High-accuracy magnetic position encoder”, *IEEE Trans. on I.A.*, Vol 35, No 3, pp 568–576, 1999.
- [19] R. Lewis, “Optimal estimation with an introduction to stochastic control theory”, John Wiley & Sons, Inc. 1986.
- [20] Q. Lin, T. Li, Z. Zhou, S. Wang, H. Guo, “Application of the magnetic encoder in actuator servo system”, *Proc IEEE ICMA 2007*, pp 3031–3035, 2007.
- [21] M. Mienkina, P. Pekarek, F. Dobes, “56F80x resolver driver and hardware Interface”, Freescale Semiconductor application note No 1942, august 2005.
- [22] M.S. Santina, A.R. Stubberud, G.H. Hostetter, “Discrete-time equivalents to continuous-time systems”, in *The control handbook* (W.S. Levine ed.), chap. 13, pp 265–279, CRC Press, 1996.
- [23] J. M. Tribolet, “A new phase unwrapping algorithm”, *IEEE Trans. on ASSP*, Vol. 25, No 2, pp 170–177, april 1977.
- [24] W.A. Wolovich, “Controllability and observability”, in *The control handbook* (W.S. Levine ed.), chap. 8.2, pp 121–130, CRC Press, 1996.